Article

Effelsberg Monitoring of a Sample of RadioAstron Blazars

Jun Liu [1,2,3,*], Thomas P. Krichbaum[1], Xiang Liu [2,3], Alex Kraus[1], Hayley Bignall[4], Yuri Y. Kovalev[5,6,1], Kirill V. Sokolovsky[7,8,5] and J. Anton Zensus[1]

1 Max-Planck-Institut für Radioastronomie, Auf dem Hügel 69, D-53121 Bonn, Germany
2 Xinjiang Astronomical Observatory, CAS, 150 Science 1-Street, Urumqi 830011, P. R. China
3 Key Laboratory of Radio Astronomy, Chinese Academy of Sciences, Urumqi 830011, P. R. China
4 CSIRO Astronomy and Space Science, 26 Dick Perry Avenue, Kensington, WA 6151, Australia
5 Astro Space Center of Lebedev Physical Institute, Profsoyuznaya 84/32, 117997 Moscow, Russia
6 Moscow Institute of Physics and Technology, Dolgoprudny, Institutsky per., 9, Moscow, Russia
7 IAASARS, National Observatory of Athens, Vas. Pavlou & I. Metaxa, 15236 Penteli, Greece
8 Sternberg Astronomical Institute, Moscow State University, Universitetskii pr. 13, 119992 Moscow, Russia
* Correspondence: jliu@mpifr-bonn.mpg.de

Abstract: The launch of the RadioAstron space radio telescope provides a unique opportunity to study the extreme high brightness temperature of Active Galactic Nuclei (AGNs) with unprecedented long baselines of up to 28 Earth diameters. A coordinated ground-based flux density monitoring of RadioAstron targets is essential to determine the effect of interstellar scintillation (ISS) on the Space Very Long Baseline Interferometry (SVLBI) visibilities. Moreover, a combination/comparison of scintillation with SVLBI observations is expected to reveal the relative influence of source brightness temperature, compactness, and properties of the interstellar medium on the observed variability at centimeter wavelengths. In 2014 we started a RadioAstron target triggered flux monitoring with the Effelsberg 100-m radio telescope in support of this SVLBI mission. A total of 112 targets were observed during the five-session monitoring performed so far. In this paper we present a statistical study on the short-term flux density variability of the sample, which is focused on the variability characteristics and derived physical properties of the observed sources.

Keywords: galaxies; active – method; statistical – radio continuum; ISM

1. Introduction

The so-called 'intra-day variability' (IDV) is the rapid flux density variability on timescales of the order of a day or less in compact extra-galactic radio sources, first discovered in the mid 1980s using the Effelsberg 100-m Radio Telescope [1,2]. Variability surveys of large source samples show that IDV is present in a significant fraction (∼20%-50%) of flat-spectrum radio sources (eg. Quasars and BL Lac objects) [3,4]. Over the past two decades, it has been established that this rapid variability is predominantly caused by scattering of radio waves through turbulent ionized structures in the Milky Way Galaxy [e.g. 5–10].

IDV sources are of astrophysical interest because the small angular sizes (no larger than tens of μas; see, e.g. [5,11,12]) they must possess in order to exhibit interstellar scintillation (ISS) requires brightness temperatures (T_B) near or, in some cases, several orders of magnitude in excess of the 10^{12}K inverse Compton limit [13]. Thanks to the unprecedented long baseline of the RadioAstron space radio telescope, we are now enabled to study the T_B of Active Galactic Nuclei (AGNs) up to 10^{15}-10^{16}K. Actually the RadioAstron AGN survey has already discovered T_B well in excess of the inverse-Compton limit in some sources, e.g. a measured $T_B \sim 10^{14}$K for 3C273 [14]. The observed excess may be either due to a very high Doppler boosting or to the violation of the inverse Compton limit. IDV observations, which are performed close in time to RadioAstron Space Very Long Baseline

Interferometry (SVLBI) observations, will benefit from the source angular scale directly measured by the latter, and could thus shed further light on the relationship between high T_B and ISS.

Aiming at a more detailed understanding of the ultra-compact component and its extreme high brightness temperature in IDVs, in 2014 we initiated a project to monitor a sample of RadioAstron blazars with the Effelsberg 100-m radio telescope. In this paper we focus on the statistics of the short-term variability from this single dish flux density monitoring.

2. Sample Selection, Observations and Data Calibration

So far five sessions of monitoring have been performed. For each observing session, the main targets were chosen from the RadioAstron block schedule. In order to enable high precision flux density measurements, a nearby non-variable calibrator was selected for each target based on the result of an IDV survey with the Urumqi 25-m radio telescope [15, in preparation] as well as the MASIV survey [16]. A few sources of particular interest were occasionally added to the list as well. With this procedure of source selection, the final source number in each session is ∼40, and the final sample size for the whole campaign is 112.

Since all the sources are point-like to the beam of the Effelsberg radio telescope at 4.85 GHz, the observations were performed in cross-scan mode, where the antenna beam pattern was driven twice in both azimuth and elevation over the source position. A duty cycle consisted of the observation of the target sources as well as their nearby non-variable secondary calibrators (e.g. 0836+710 and 0951+699). The average duty cycle is 0.4 h^{-1} in the campaign, which translates into an average time sampling of ∼2.5 hours for each source.

Frequent switching between targets and calibrators allowed monitoring of the antenna gain variations with elevation and time, thus improving the subsequent flux density calibration. The data calibration was done in the well established, standard manner, and enabled to achieve high precision flux density measurements. In short, it consists of the following steps: after a Gaussian fitting, corrections are computed for antenna pointing offsets, gain-elevation and gain-time effects; then, the measured antenna temperature is converted to an absolute flux density by utilizing the frequently observed primary calibrators 3C286, 3C48 and NGC7027. The efficiency of this standard procedure can be evaluated by measuring the residual scatter, m_c, in the data of the calibrators (see definition in section 3). For most of the observation sessions, the residual scatter is 0.3 – 0.5%.

3. Variability Parameters

A number of parameters are defined to characterize the variability. For each light curve the 'raw' modulation index m, 'intrinsic' modulation index $\overline{m}$ and reduced χ^2 are derived. A brief definition and description of these quantities is given here, the reader is referred to e.g. [17,18] for more details.

The raw modulation index is related to the standard deviation of the flux density Δ_S and the mean value of the flux density $\langle S \rangle$ in the time series by

$$m[\%] = 100 \cdot \frac{\Delta_S}{\langle S \rangle} \tag{1}$$

and yields a measure for the strength of the observed variations. The value of raw modulation index for all the observed non-variable calibrators (m_c) usually represents the calibration accuracy. The intrinsic modulation index $\overline{m}$ [see 18, and reference therein] is an alternative estimator to quantify the variability that would be observed in the absence of measurement errors and with ideal time sampling. Note that this use of 'intrinsic' is not referring to source-intrinsic variability, but includes any intrinsic and extrinsic (ISS-induced) variations in the received flux density. The definition of $\overline{m}$ involves a two-dimensional maximum-likelihood function

$$\mathscr{L}(\overline{m}, S_0) = S_0 \left(\prod_{j=1}^{N} \frac{1}{\sqrt{2\pi \left(\overline{m}^2 S_0^2 + \sigma_j^2 \right)}} \right) \exp \left(-\frac{1}{2} \sum_{j=1}^{N} \frac{\left(S_j - S_0 \right)^2}{\overline{m}^2 S_0^2 + \sigma_j^2} \right) \tag{2}$$

where S_0 is the average source flux density, S_j the individual flux density measurements, σ_j their errors and N the number of measurements. Furthermore, as a criterion to identify the presence of variability, the null-hypothesis of a constant function is examined via a χ^2-test

$$\chi^2 = \sum_{j=1}^{N} \left(\frac{S_j - \langle S \rangle}{\sigma_j} \right)^2 \tag{3}$$

and the reduced value of χ^2

$$\chi_r^2 = \frac{1}{N-1} \sum_{j=1}^{N} \left(\frac{S_j - \langle S \rangle}{\sigma_j} \right)^2 \tag{4}$$

A source is classified as variable if the χ^2-test gives a probability of $< 0.01\%$ for the assumption of constant flux density (99.99% significance level for variability).

4. Results and Discussion

Of the 112 targets observed, 33 sources exhibited IDV in at least one observing epoch, while 79 sources didn't show evident short-term variability in any epoch. This leads to an IDV detection rate of $\sim$30% in our monitoring sample, consistent with earlier studies [3,4]. Of the 54 sources with a Gev detection by Fermi, 24 showed IDV, indicating that almost half of the γ-ray loud sources are variable at cm-wavelength. By contrast the ratio is $\sim$16% for γ-ray quiet sources. A summary for this result is given in Table 1 and Figure 1, showing clearly the higher fraction of the occurrence of IDV in γ-ray loud sources.

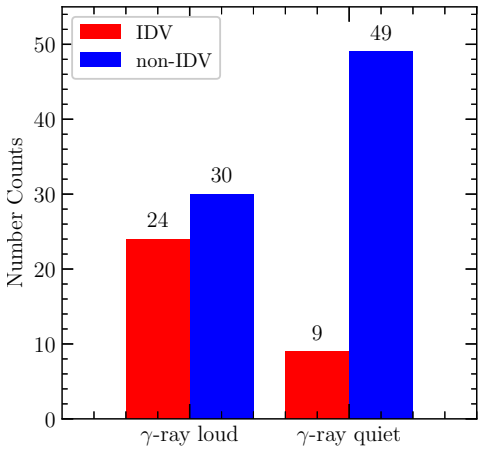

Figure 1. The occurrence of IDV and non-IDV in γ-ray loud/quiet subsamples, respectively.

Table 1. Overall statistics concerning the IDV detection rate in different classes of sources.

var. status	γ-ray loud	γ-ray quiet	total
IDV	24	9	33
non-IDV	30	49	79
total	54	58	112

4.1. the Intrinsic Modulation Index $\overline{m}$

We first investigate the distribution of the intrinsic modulation index $\overline{m}$, as it's essential for subsequent population studies. The probability density of $\overline{m}$ (note a median value is taken if the source was observed in multiple epochs) is plotted in Figure 2. The distribution can be well characterized by an exponential function defined as $f(\overline{m})d\overline{m} = \frac{5}{4m_0} exp(-\frac{5\overline{m}}{4m_0})dm$ with m_0 the mean of $\overline{m}$. The red dashed line represents an exponential distribution of mean m_0 = 0.78% which, as we can see, is an excellent description of the data.

Furthermore, by utilizing the formalism introduced in Section 6.3.3 of Richards *et al.* [18], we will be able to study the possible correlations between the intrinsic modulation index $\overline{m}$ and physical properties in our sample. This will be done by testing whether the distributions of $\overline{m}$ in subsets of our sample split according to some source property are consistent with each other. The applications of these population studies are presented in the following subsections.

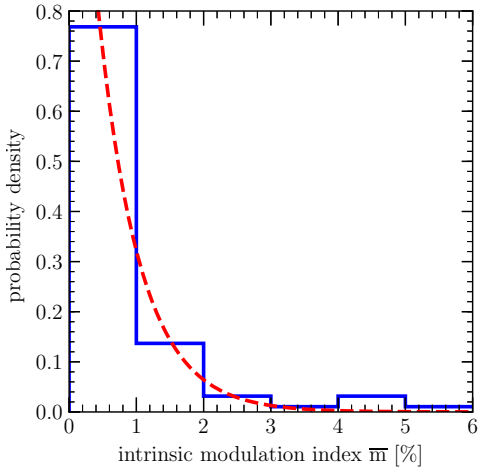

Figure 2. Probability density of the maximum-likelihood intrinsic modulation indices $\overline{m}$. The red dashed line represents an exponential distribution with m_0=0.78%.

4.2. Flux Density

In this subsection we test the dependence of variability on source flux density, which is tightly bounded with source angular diameter, if the brightness temperature is inverse Compton limited. A population study is performed to examine subsets defined by whether the source flux density is higher or lower than 1 Jy (note a median value is taken if the source was observed in multiple epochs). The results of this test are displayed in Figure 3. In the left panel, it is obvious that the curves for these two subsamples are not consistent with each other – weaker sources have, on average, higher variability amplitude. This trend is expected for a brightness temperature limited sample, as the stronger sources have larger angular size, suppressing the ISS. This finding is verified by the right panel of Figure 3, in which the probability density of the difference between the m_0 of weak and strong sources is plotted. The most likely difference is 1.16 percentage points, and it is more than 5σ away from zero.

4.3. Spectral Index

Early observations showed that scintillating sources tend to have flat or inverted spectra, while the steep-spectrum radio sources do not scintillate [19]. This can be understood by considering that the flat-spectrum sources are dominated by optically thick, synchrotron self-absorbed components with very high-brightness temperature, thus most of their flux density is confined to the ultra-compact core regions. In contrast, the steep-spectrum sources are dominated by optically thin, less compact emission with lower brightness temperatures, often related to an extended VLBI jet.

Preprints (www.preprints.org) | NOT PEER-REVIEWED | Posted: 31 October 2017 doi:10.20944/preprints201710.0191.v1

Peer-reviewed version available at Galaxies 2018, 6, 49; doi:10.3390/galaxies6020049

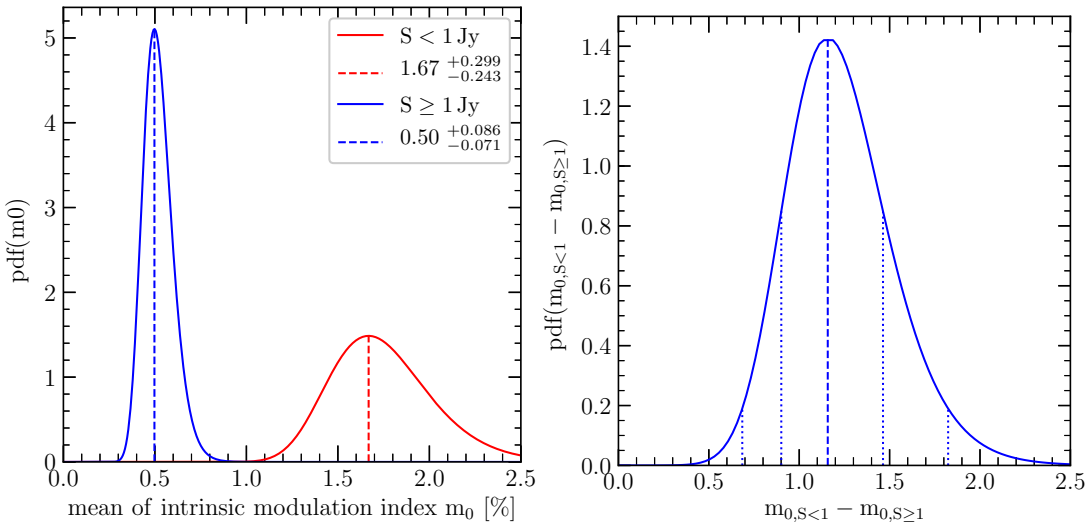

Figure 3. Left panel: Probability density of m_0 for sources with flux density lower (red solid line, maximum-likelihood value and 1σ error $m_0 = 1.67^{+0.299}_{-0.243}$%) and higher (blue solid line, maximum-likelihood value and 1σ error $m_0 = 0.5^{+0.086}_{-0.071}$%) than 1 Jy in our monitoring sample. The dashed vertical lines locate the peaks of probability density for the two subsamples. Right panel: Probability density of the difference between the m_0 for the two sets considered in the right panel. The dashed vertical line locates the peak of the probability density, while the dotted vertical lines represents the 1, 2 and 3σ confidence interval. The peak of the distribution ($1.16^{+0.303}_{-0.259}$) is over 5σ away from zero.

To test this argument, we split the sample at $\alpha = -0.1$ (defined by $S \propto \nu^{\alpha}$). This criterion roughly splits our sample between flat and inverted spectrum, and produces similarly sized subsamples. Figure 4 shows the probability distributions of m_0 as well as the difference between m_0 for these two subsamples. The result, as anticipated, suggests that sources with inverted spectra are significantly ($\geq 6\sigma$) stronger in short-term variability. It has to be noted, however, that the sources in the present sample are mostly compact, core-dominated sources with flat spectrum, unlike the classical steep-spectrum sources reported by Heeschen [19] which are dominated by their extended emission. Our findings indicate that even for the flat spectrum sources the presence of less compact components could in principle reduce their compact fractions thus suppressing the scintillation.

4.4. γ-ray Loudness

The connection between the radio and γ-ray emission in blazars has been extensively studied, especially in the Fermi era [e.g. 20–23]. The investigation of fast variability for the γ-ray loud sources in the radio bands is usually performed through the cross-correlation between the multi-frequency lightcurves. If such correlation is confirmed, the site of the γ-ray emitting region can be located [e.g. 24]. In this study we test, through a statistical approach, the existence of a connection between the γ-ray properties and the radio compactness.

We thus divide our sample in two subsets, based on whether the source has been detected by Fermi LAT at a significance level high enough to warrant inclusion in the 3FGL catalog. As shown in Figure 5, these two subsamples show different properties: the γ-ray loud sources have, on average, a variability amplitude almost a factor of four higher than γ-ray quiet ones. The result is very significant statistically, with the maximum-likelihood difference being 7σ away from 0, as indicated in the right panel of Figure 5.

4.5. Galactic Latitude and k-index

We have also investigated how the galactic latitude is related to source variability. In case of ISS, a galactic latitude dependence of variability is anticipated, since the diffuse interstellar medium (ISM)

Preprints (www.preprints.org) | NOT PEER-REVIEWED | Posted: 31 October 2017 doi:10.20944/preprints201710.0191.v1

Peer-reviewed version available at Galaxies 2018, 6, 49; doi:10.3390/galaxies6020049

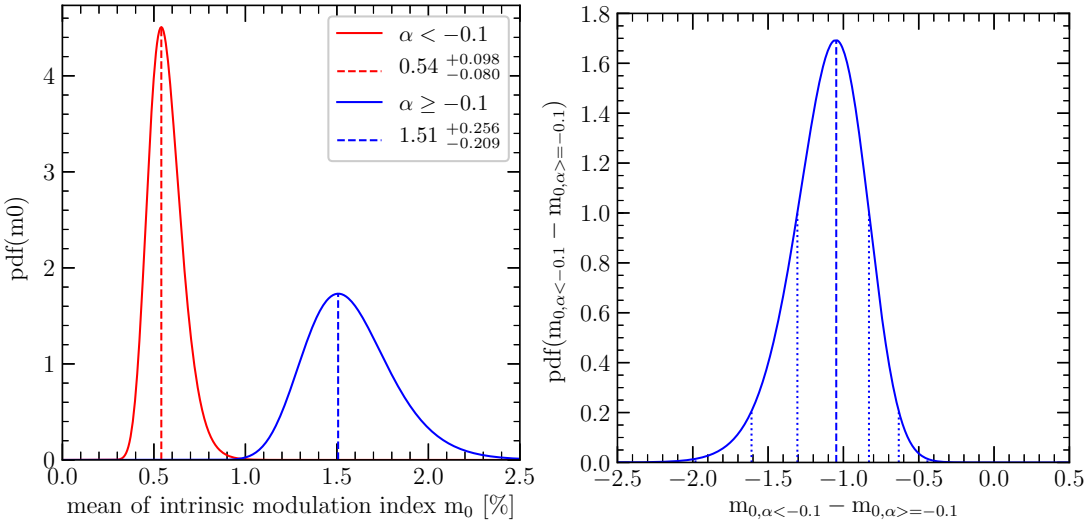

Figure 4. Similar as Figure 3 but for sources with spectral index lower (red solid line) and higher (blue solid line) than -0.1. In the left panel the maximum-likelihood value and the associated 1σ error are indicated in the legend. In the right panel the peak of the distribution ($-1.05^{+0.217}_{-0.258}$) is over 6σ away from zero.

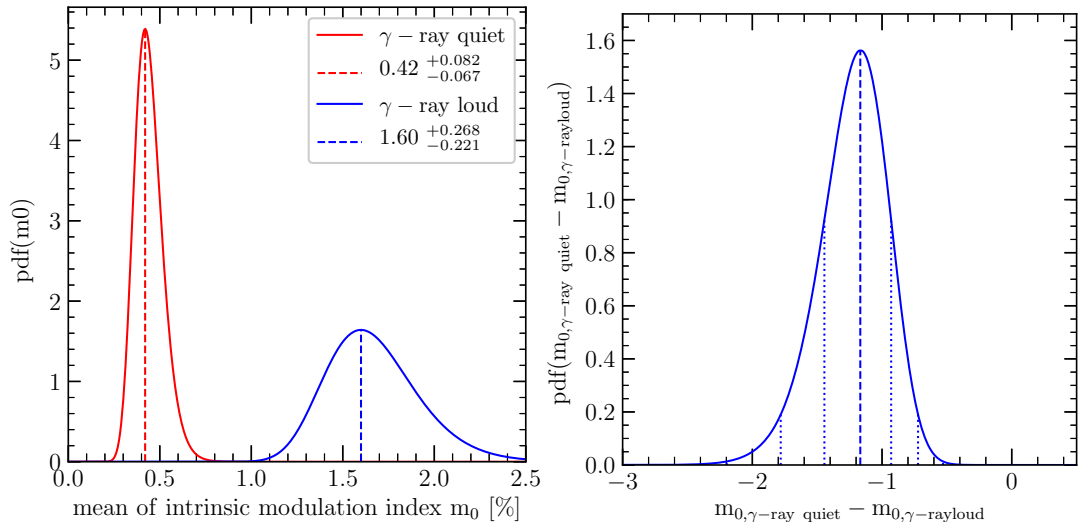

Figure 5. Similar as Figure 3 but for γ-ray quiet (red solid line) and γ-ray loud (blue solid line) sources. In the left panel the maximum-likelihood value and the associated 1σ error are indicated in the legend. In the right panel the peak of the distribution ($-1.17^{+0.238}_{-0.276}$) is $\sim 7\sigma$ away from zero.

are mostly distributed near the galactic plane. However only week dependence of this nature has been observed so far [16,25]. A contingency test dividing the sample into a low and high galactic latitude subsamples at $|b| = 20^\circ$ shows that the two distributions of m_0 are rather consistent with each other. The probability density for the difference between m_0 for the two subsamples is consistent with zero to within 1σ (see Figure 6). Hence our result doesn't support the previous findings mentioned above.

In order to verify this result, we alternatively test the role of the k-index in the fast variability. The k-index is a power-law index that describes how the source angular size scales with frequency through $\theta \propto \nu^{-k}$, $k = \frac{\beta}{\beta-2}$ [26,27, and reference therein], where β is the index of the assumed power-law spectrum of the turbulent electron density fluctuations. For turbulence with Kolmogorov spectrum, $\beta = 11/3$ is expected. In this case, the scattered angular size of a source is proportional to $\nu^{-2.2}$. While if no scattering is present, the observed angular size is expected to scale approximately as ν^{-1}.

Preprints (www.preprints.org) | NOT PEER-REVIEWED | Posted: 31 October 2017 doi:10.20944/preprints201710.0191.v1

Peer-reviewed version available at Galaxies 2018, 6, 49; doi:10.3390/galaxies6020049

The value of k-index therefore, provides an estimation of the strength of angular broadening due to interstellar scattering. A recent statistical study on AGN cores reveals a bimodal distribution of k-index for sources with galactic latitude $|b| < 10°$, indicating that the angular scatter-broadening is partially present in low galactic latitude sources [28].

With the k values provided in Pushkarev and Kovalev [28], our sample is then subdivided into scattering and non-scattering subsets at k=1.1. As shown in Figure 7 the distributions of m_0 are quite consistent with each other. The most likely difference is 0.06 percentage, which is very close to zero and obviously located within the 1σ confidence interval. This confirms the result on galactic latitude.

The lack of correlation of short timescale variability strength with Galactic latitude and k-index could be ascribed to two competitive effects related to the distance to and path length through the ISM [4, and reference therein]. On the one hand, the increased path length makes the scintillation stronger at lower latitudes so that the intrinsic modulation index should increase. On the other hand, the increased distance slows the scintillation time, which may cause a decrease in variability strength estimation. Moreover, extreme variability usually occurs where there happens to be a relatively nearby scattering 'screen' [see, e.g. 29]. In that case, ISS is less quenched than for a more distant screen for a source of a given angular diameter.

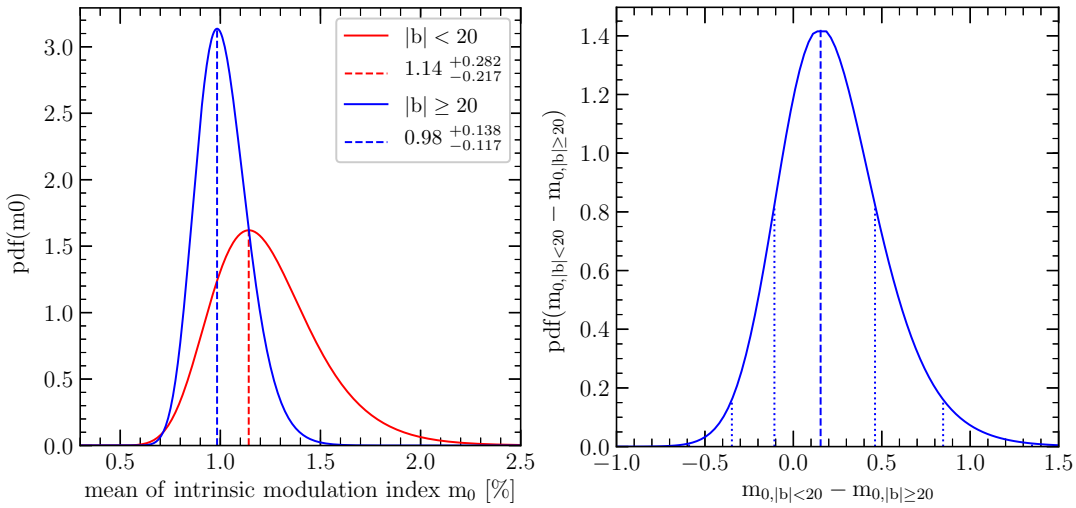

Figure 6. Similar as Figure 3 but for low (red solid line) and high (blue solid line) galactic latitude sources in our sample. In the left panel the maximum-likelihood value and the associated 1σ error are indicated in the legend. In the right panel the peak of the distribution ($0.15^{+0.312}_{-0.257}$) is consistent with zero within 1σ.

5. Summary and Conclusion

We presented the statistical results based on the five sessions of AGN monitoring with the Effelsberg 100-m radio telescope. The overall statistics showed that 33 out of 112 sources exhibited IDV, leading to an IDV detection rate of ∼30%. The IDV occurrence for γ-ray loud sources is ∼44%, which is significantly higher than that for the γ-ray quiet ones.

Moreover, with a maximum-likelihood approach we investigated the variability dependence of our sample. We found significant difference in variability strength when regarding the source flux density, spectral index and γ-ray loudness. In more detail, weak (S < 1 Jy), inverted spectrum ($\alpha > -0.1$) or γ-ray loud sources, on average, show significantly stronger short timescale variability. The most likely differences in mean m_0 are at least 5σ away from zero. On the other hand, however we didn't find evident dependence of variability on galactic latitude and k-index. This might suggest that sources dominated by scatter-broadening effect are more likely to show refractive ISS, which is on timescales significantly longer than a few days.

Preprints (www.preprints.org) | NOT PEER-REVIEWED | Posted: 31 October 2017 doi:10.20944/preprints201710.0191.v1

Peer-reviewed version available at Galaxies 2018, 6, 49; doi:10.3390/galaxies6020049

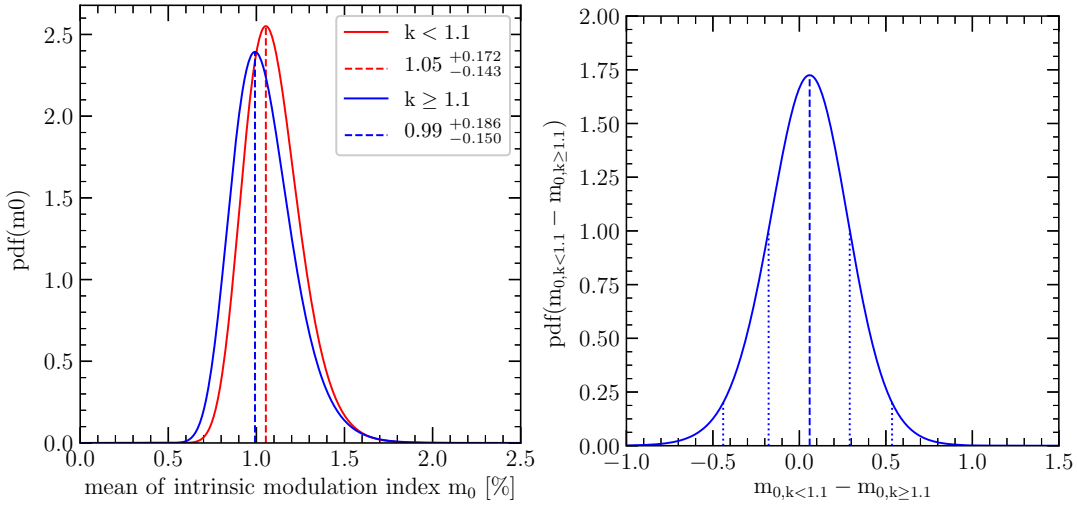

Figure 7. Similar as Figure 3 but for sources with *k*-index lower (red solid line) and higher (blue solid line) than 1.1 in our sample. In the left panel the maximum-likelihood value and the associated 1σ error are indicated in the legend. In the right panel the peak of the distribution ($0.06^{+0.231}_{-0.238}$) is consistent with zero within 1σ.

By testing the variability strength in different subsets, the current study indicates a source compactness dependent variability in the sample. Future studies on this issue are needed, and these will doubtless well benefit from the VLBI core angular size and core dominance directly measured by the RadioAstron SVLBI observations.

Acknowledgments: The authors thank Dr. Biagina Boccardi for reviewing the manuscript and providing helpful comments. This paper made use of data obtained with the 100-m telescope of the MPIfR (Max-Planck-Institut für Radioastronomie) at Effelsberg. This research was partially supported by the program of the Light in China's Western Region (Grant No. 2015-XBQN-B-01, YBXM-2014-02, XBBS201324), the National Natural Science Foundation of China (NSFC, Grant No. 11503071, 11503072), the National Basic Research Program of China (973 program, Grant No. 2015CB857100), Xinjiang Key Laboratory of Radio Astrophysics (Grant No. 2016D03020) and the China Scholarship Council (CSC, Grant No. 201704910392). YYK acknowledges support by the government of the Russian Federation (agreement 05.Y09.21.0018) and the Alexander von Humboldt Foundation.

Conflicts of Interest: The authors declare no conflict of interest.

References

1. Witzel, A.; Heeschen, D.S.; Schalinski, C.; Krichbaum, T. Kurzzeit-Variabilität extragalaktischer Radioquellen. *Mitteilungen der Astronomischen Gesellschaft Hamburg* **1986**, *65*, 239.
2. Heeschen, D.S.; Krichbaum, T.; Schalinski, C.J.; Witzel, A. Rapid variability of extragalactic radio sources. AJ **1987**, *94*, 1493–1507.
3. Quirrenbach, A.; Witzel, A.; Kirchbaum, T.P. et al. Statistics of intraday variability in extragalactic radio sources. A&A **1992**, *258*, 279–284.
4. Lovell, J.E.J.; Rickett, B.J.; Macquart, J.P. et al. The Micro-Arcsecond Scintillation-Induced Variability (MASIV) Survey. II. The First Four Epochs. ApJ **2008**, *689*, 108–126, [0808.1140].
5. Kedziora-Chudczer, L.; Jauncey, D.L.; Wieringa, M.H. et al. PKS 0405-385: The Smallest Radio Quasar? ApJ **1997**, *490*, L9–L12, [astro-ph/9710057].
6. Jauncey, D.L.; Macquart, J.P. Intra-day variability and the interstellar medium towards 0917+624. A&A **2001**, *370*, L9–L12, [astro-ph/0102194].
7. Dennett-Thorpe, J.; de Bruyn, A.G. Interstellar scintillation as the origin of the rapid radio variability of the quasar J1819+3845. Nature **2002**, *415*, 57–60, [astro-ph/0201061].
8. Bignall, H.E.; Jauncey, D.L.; Lovell, J.E.J. et al. Rapid Variability and Annual Cycles in the Characteristic Timescale of the Scintillating Source PKS 1257-326. ApJ **2003**, *585*, 653–664, [astro-ph/0211451].

9. Bignall, H.E.; Macquart, J.P.; Jauncey, D.L. et al. Rapid Interstellar Scintillation of PKS 1257-326: Two-Station Pattern Time Delays and Constraints on Scattering and Microarcsecond Source Structure. ApJ **2006**, *652*, 1050–1058, [astro-ph/0608619].
10. Liu, B.R.; Liu, X.; Marchili, N. et al. Two-year monitoring of intra-day variability of quasar 1156+295 at 4.8 GHz. A&A **2013**, *555*, A134, [arXiv:astro-ph.HE/1305.5612].
11. Savolainen, T.; Kovalev, Y.Y. Serendipitous VLBI detection of rapid, large-amplitude, intraday variability in QSO 1156+295. A&A **2008**, *489*, L33–L36, [0809.0451].
12. Liu, J.; Liu, X. Rapid variability of BL Lac 0925+504: interstellar scintillation induced? Ap&SS **2015**, *357*, 165.
13. Kellermann, K.I.; Pauliny-Toth, I.I.K. The Spectra of Opaque Radio Sources. ApJ **1969**, *155*, L71.
14. Kovalev, Y.Y.; Kardashev, N.S.; Kellermann, K.I. et al. RadioAstron Observations of the Quasar 3C273: A Challenge to the Brightness Temperature Limit. ApJ **2016**, *820*, L9, [arXiv:astro-ph.HE/1601.05806].
15. Liu, J.; Liu, X.; Krichbaum, T.P. et al. UNSS: The Urumqi Northern Sky Survey for Rapid Variability in Compact Radio Sources. ApJ **2017**.
16. Lovell, J.E.J.; Jauncey, D.L.; Bignall, H.E. et al. First Results from MASIV: The Microarcsecond Scintillation-induced Variability Survey. AJ **2003**, *126*, 1699–1706, [astro-ph/0306484].
17. Fuhrmann, L.; Krichbaum, T.P.; Witzel, A. et al. Testing the inverse-Compton catastrophe scenario in the intra-day variable blazar S5 0716+71. III. Rapid and correlated flux density variability from radio to sub-mm bands. A&A **2008**, *490*, 1019–1037, [0809.2227].
18. Richards, J.L.; Max-Moerbeck, W.; Pavlidou, V. et al. Blazars in the Fermi Era: The OVRO 40 m Telescope Monitoring Program. ApJS **2011**, *194*, 29, [arXiv:astro-ph.CO/1011.3111].
19. Heeschen, D.S. Flickering of extragalactic radio sources. AJ **1984**, *89*, 1111–1123.
20. Ghirlanda, G.; Ghisellini, G.; Tavecchio, F.; Foschini, L. Correlation of Fermi Large Area Telescope sources with the 20-GHz Australia Telescope Compact Array radio survey. MNRAS **2010**, *407*, 791–803, [arXiv:astro-ph.HE/1003.5163].
21. Ackermann, M.; Ajello, M.; Allafort, A. et al. The Radio/Gamma-Ray Connection in Active Galactic Nuclei in the Era of the Fermi Large Area Telescope. ApJ **2011**, *741*, 30, [arXiv:astro-ph.CO/1108.0501].
22. Migliori, G.; Siemiginowska, A.; Kelly, B.C. et al. Jet Emission in Young Radio Sources: A Fermi Large Area Telescope Gamma-Ray View. ApJ **2014**, *780*, 165, [arXiv:astro-ph.HE/1311.7647].
23. Richards, J.L.; Hovatta, T.; Max-Moerbeck, W. et al. Connecting radio variability to the characteristics of gamma-ray blazars. MNRAS **2014**, *438*, 3058–3069, [arXiv:astro-ph.HE/1312.3634].
24. Fuhrmann, L.; Larsson, S.; Chiang, J. et al. Detection of significant cm to sub-mm band radio and γ-ray correlated variability in Fermi bright blazars. MNRAS **2014**, *441*, 1899–1909, [arXiv:astro-ph.HE/1403.4170].
25. Lazio, T.J.W.; Ojha, R.; Fey, A.L. et al. Angular Broadening of Intraday Variable AGNs. II. Interstellar and Intergalactic Scattering. ApJ **2008**, *672*, 115–121, [0707.1778].
26. Rickett, B.J. Interstellar scattering and scintillation of radio waves. ARA&A **1977**, *15*, 479–504.
27. Pushkarev, A.B.; Kovalev, Y.Y.; Lister, M.L. et al. VLBA observations of a rare multiple quasar imaging event caused by refraction in the interstellar medium. A&A **2013**, *555*, A80, [arXiv:astro-ph.CO/1305.6005].
28. Pushkarev, A.B.; Kovalev, Y.Y. Milky Way scattering properties and intrinsic sizes of active galactic nuclei cores probed by very long baseline interferometry surveys of compact extragalactic radio sources. MNRAS **2015**, *452*, 4274–4282, [arXiv:astro-ph.HE/1507.02459].
29. Walker, M.A.; Tuntsov, A.V.; Bignall, H. et al. Extreme Radio-wave Scattering Associated with Hot Stars. ApJ **2017**, *843*, 15, [1705.00964].